

# STUDY ON CONTROL AND STABILITY OF THE ROCKET PLANE TO SPACE TOURISM

**Agnieszka Kwiek**  
**Warsaw University of Technology**  
**Institute of Aeronautics and Applied Mechanics**

**Keywords:** *static stability, pitching channel control, rocket plane, LEX*

## Abstract

*This paper presents study of control and the static stability of a rocket plane. The vehicle is been designed for a suborbital space tourism. The concept of the rocket plane control assumes two types of control surfaces. The first involves two segmented elevons. The second involves rotating side plates on the wing tips. The presented results are focused on the longitudinal static stability and the control of a pitching channel.*

*CFD calculations were conducted by ANSYS Flunet 14.0 and MGAERO software. The paper presents diagrams of lift versus drag coefficient for trim conditions for subsonic and supersonic speeds. Derivatives of lift and pitching coefficients in respect to control surfaces deflection are also included.*

## 1 Introduction

Suborbital space flights are a very promising idea. There are a few possible applications of this kind of flights [1]. The most attractive is space tourism. Nowadays is the cheapest way to visit the outer space. Currently a few companies are working on the first manned commercial vehicle to be used in the suborbital space flights. Moreover, the suborbital vehicle can be used as a way to put micro satellites into low Earth orbit. In that case on board of a suborbital vehicle there must be additional device which will release the micro satellite, when an orbit is achieved [2]. It presents great opportunity to launch satellites for countries which do not have rocket programs or lunch facilities. The next possible application

is use of suborbital space vehicles as a testing platform for new space technology and to improve Technology Readiness Level (TRL). Finally, suborbital flights are a possible way for a fast point to point travel in the far future [1].

### 1.1 Modular Airplane System

A Modular Airplane System (MAS) [2],[4] has been designed at the Warsaw University of Technology at the Faculty of Power and Aeronautical Engineering. The main application of MAS is suborbital manned flights. The MAS consists of a Carrier and a Rocket Plane. Both vehicles have tailless configuration, but bonded together form a conventional airplane where the Rocket Plane is used as a tail of the MAS.

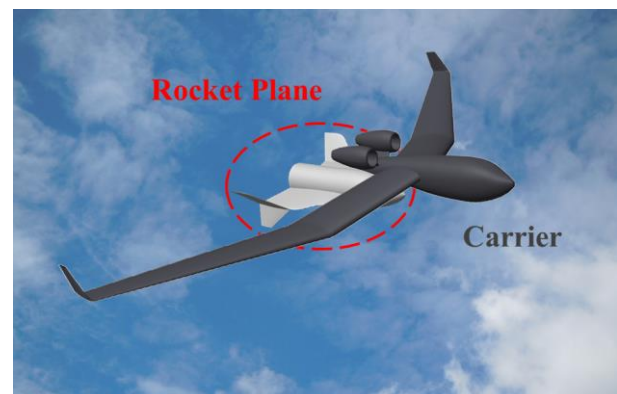


**Fig. 1 Layout of the Modular Airplane System.**

The mission profile of the MAS is presented in Fig. 2. Results presented in this paper concern only selected parts of the Rocket Plane mission.

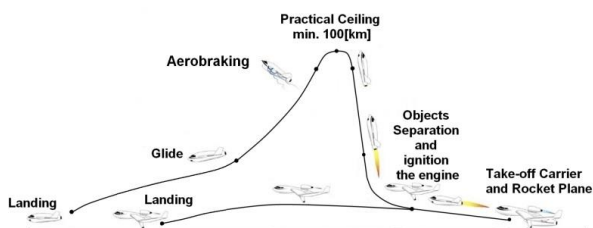


**Fig. 2 MAS mission profile**

Results of earlier analyses for MAS are presented in [2]- [7].

**2 Rocket Plane**

The Rocket Plane is design in a tailless configuration and consists of a fuselage, a delta wing, side plates and a LEX (Leading Edge Extension) [8]. The fuselage has circular cross-section. The down side's plates were added because solve problem with directional stability. The shape of the Rocket Plane's LEX is the result of the optimization process. The LEX will generate a lift vortex [8] which in turn reduces a rate of descent during the return phase. The initial re-entry speed of the vehicle should be small, therefore the problem of structure overheating should not occur.

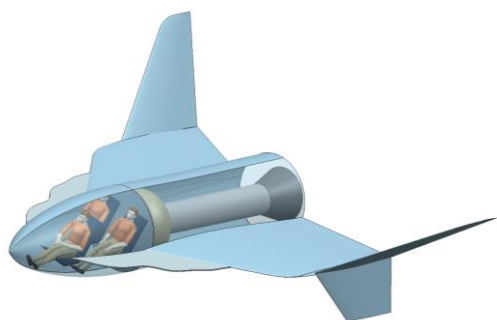


**Fig. 3 Rocket Plane layout**

**2.1 Concept of control**

A concept of the Rocket Plane control assumes two types of control surfaces (see Fig. 4). The first one is elevons which are extended along almost the whole wing span and take exactly 30% of a local chord. Moreover, the elevons are divided into two equal span segments which can be independently deflected.

The second types of control surfaces are the rotating side plates (all moving tail) placed

on the wing tips. The axis of rotation of the all moving tail is presented in Fig. 4. In addition different dihedral angles of the all moving tail were considered (see Fig. 5).

The two segmented elevons are used in control of a pitching and rolling moment. However the all moving tail is used in control of a pitching and yawing moment. This paper is focused only on a pitching channel control.

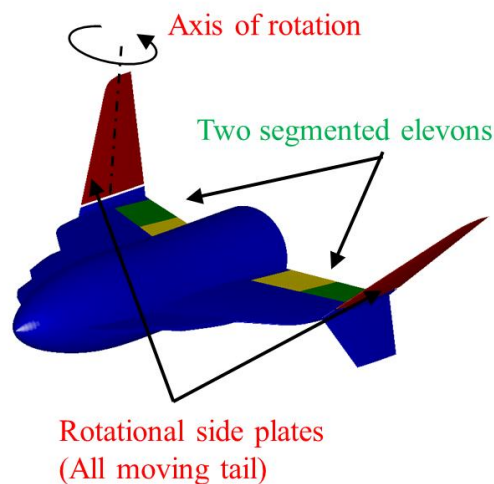


**Fig. 4 Concept of the Rocket Plane control.**

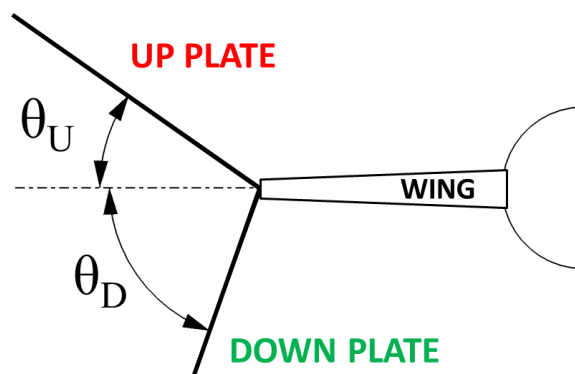


**Fig. 5 Definition of all moving tail dihedral**

The Rocket Plane should be able to fly at subsonic and supersonic speeds hence, it need for a control system which is effective for a wide range of Mach numbers. The main purpose of this research was to study possible applications of the presented concept of control in vehicles which can be used in space tourism.

### 3 CFD calculations

Two types of software were used to make CFD calculations. The first one was ANSYS Flunet 14.0 which solving Navier-Stokes equations. This software was used for subsonic cases analysis.

The second one was MGAERO which solve Euler equations (inviscid flow) and used a multi-grid scheme [9]. This software was used for supersonic calculations. Although this software can be used for vortex flow calculations, must be noted that it does not include the vortex breakdown.

Both numerical models were created for the Rocket Plane in 1:1 scale.

#### 3.1 Numerical models

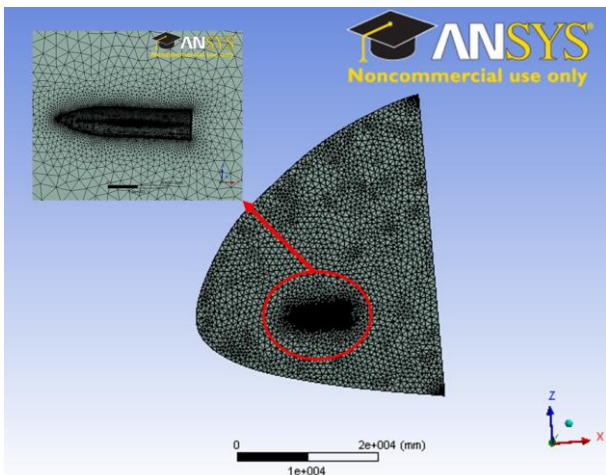


**Fig. 6 Numerical model for ANSYS Fluent computation.**

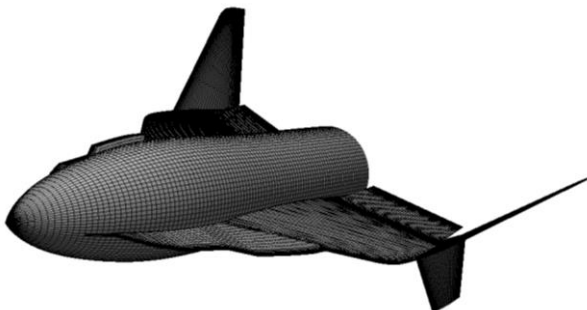


**Fig. 7 Example of grid over the Rocket Plane, numerical model for MGAERO computation**

The mesh for ANSYS Fluent calculations is presented in Fig. 6. The model

includes the mesh for boundary layer calculations. As a turbulence model the k-ε model was used.

The grid for supersonic calculation is presented in Fig. 7. Moreover, over the model seven levels of multi-grid blocks were generated.

#### 3.2 Assumptions

The subsonic calculations were made for two Reynolds numbers, for  $Re=10.5 \cdot 10^6$  and  $Re=15 \cdot 10^6$ .

The supersonic calculations were made for Mach number equal to  $Ma=1.2$

As a reference point for pitching moment calculation the position of the vehicle's center of gravity during return flight was assumed.

The presentation of results is divided into two main parts. The first one includes outcomes of subsonic calculation (paragraph no.4), the second one presents results for supersonic speed (paragraph no.5).

### 4 Results for subsonic cases

As was mentioned the analysis for subsonic speeds was made for two Reynolds numbers,  $Re=10.5 \cdot 10^6$  and  $Re=15 \cdot 10^6$ .

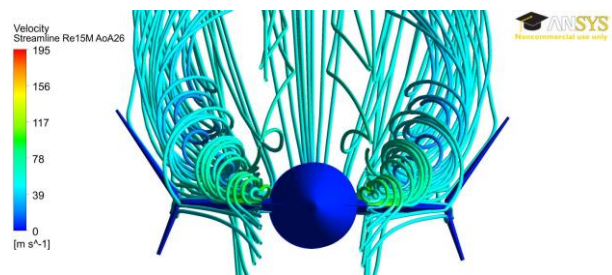


**Fig. 8 Vortex flow visualization for  $Re=15M$   $\alpha=24$  deg. and  $\delta_{EW}=-10$**

The vortex flow visualization for model with control surfaces deflected is presented in Fig. 8.

#### 4.1 Longitudinal static stability

Comparison of the pitching moment coefficient versus the angle of attack for  $Re=10.5 \cdot 10^6$  and  $Re=15 \cdot 10^6$  are presented in

Fig. 9. The shape of characteristics is similar. The Rocket Plane is statically stable between the angle of attack 0 to 8 degrees and between 28 to 42 degrees for  $Re=15 \cdot 10^6$ . However for  $Re=10.5 \cdot 10^6$ , the Rocket Plane is statically stable between the angle of attack 0 to 8 degrees and between 30 to 42 degrees.

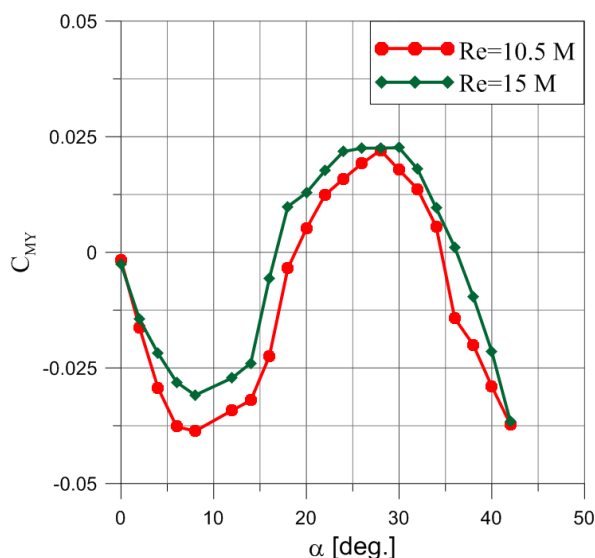


Fig. 9 Comparison of the pitching moment coefficient versus the angle of attack for subsonic cases

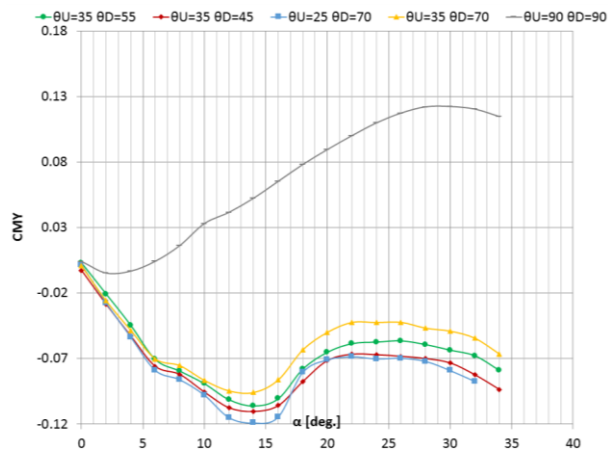


Fig. 10 Pitching moment coefficients versus the angle of attack for  $Re=10.5$  for a few all moving tail configurations

An influence of the dihedral of the all moving tail on a pitching moment characteristic is also investigated. The diagram of the pitching moment coefficient versus the angle of attack for a few configurations of the all moving tail is

presented in Fig. 10. The shapes of curves on the diagram are similar and the changing of the tail dihedral do not caused the eliminations of the unstable part of the characteristics. When the all moving tail dihedral is closer to 90 degrees, the instability is increased. If dihedral of both side plates is equal 90 degree, the Rocket Plane is unstable for almost all angles of attack (see Fig. 10)

#### 4.2 Control of the pitching channel for $Re=15 \cdot 10^6$

To obtain the trim conditions four configurations of the control surfaces deflection were analyzed:

- The all moving tail ( $\delta_R$ )
- Both segments of the elevons ( $\delta_E$ )
- The all moving tail and both segments of the elevons ( $\delta_R$  and  $\delta_E$ )
- Only inner part of the elevons ( $\delta_{EW}$ )

The lift coefficient versus drag coefficient for trim conditions is presented in Fig. 11. The diagram presents coefficients also for unstable equilibriums.

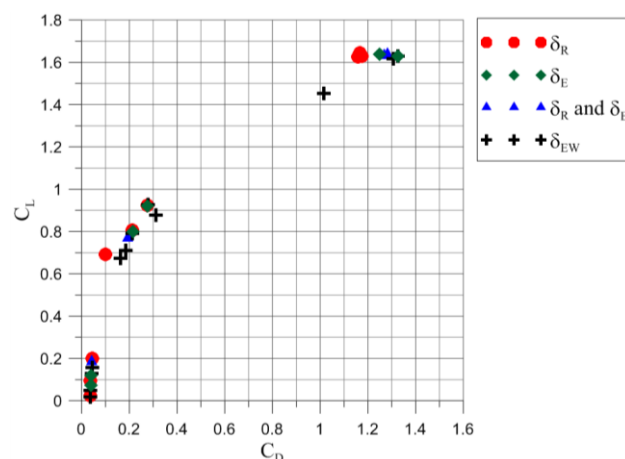
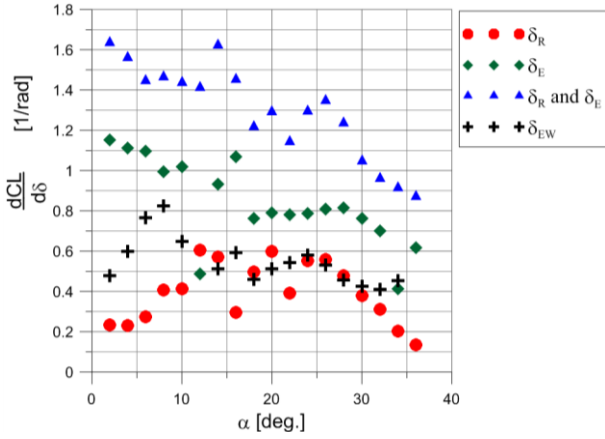


Fig. 11 The lift versus drag coefficient for trim conditions for  $Re=15 \cdot 10^6$

Derivatives of the lift in respect to the control surfaces deflection versus the angle of attack are presented in Fig. 12.



**Fig. 12 Derivative of lift coefficient in respect to control surfaces deflection versus the angle of attack for  $Re=15 \cdot 10^6$**

Derivatives of the pitching moment in respect to the control surfaces deflection versus the angle of attack are presented in Fig. 13

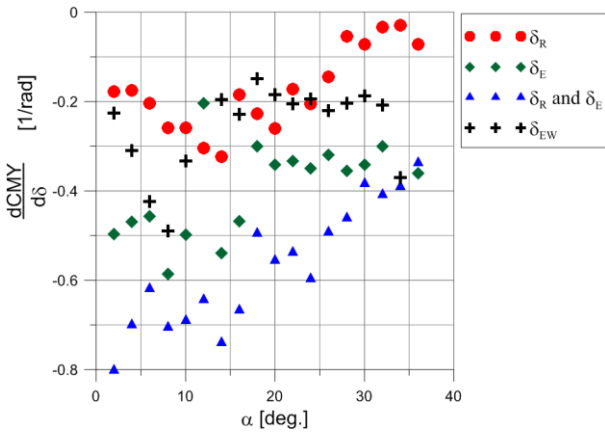


**Fig. 13 Derivative of pitching moment coefficient in respect to control surfaces deflection versus the angle of attack for  $Re=15 \cdot 10^6$**

The most effective of the control surfaces configuration is simultaneous deflection of the all moving tail and both elevon segments. The less effective case is deflection only the all moving tail.

**4.3 Control of the pitching channel for  $Re = 10.5 \cdot 10^6$**

To obtain the trim conditions four configurations of control surfaces deflection were analyzed:

- The all moving tail ( $\delta_R$ )

- The all moving tail and inner segment of the elevens ( $\delta_R$  and  $\delta_{EW}$ )
- Only inner part of the elevens ( $\delta_{EW}$ )
- Both parts of the elevens ( $\delta_E$ )

The lift coefficient versus drag coefficient for trim conditions is presented in Fig. 14. The diagram presents coefficients also for unstable equilibriums.

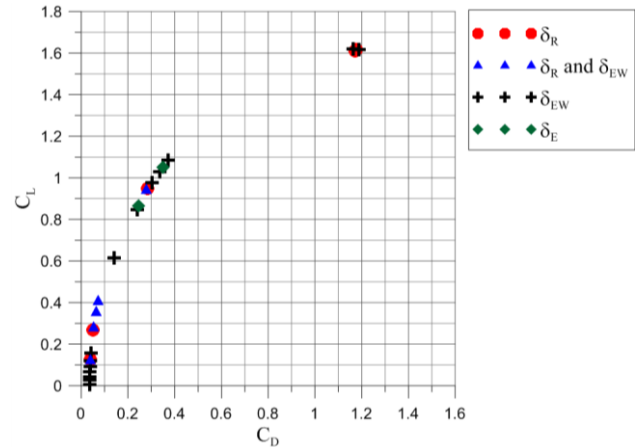


**Fig. 14 Lift versus drag coefficient for trim conditions for  $Re=10.5 \cdot 10^6$**

Moreover, the concept of obtained trim conditions by changing the all moving tail dihedral was investigated. Fig. 15 presents the lift versus drag coefficient for trim conditions completed on points for the mentioned concept.

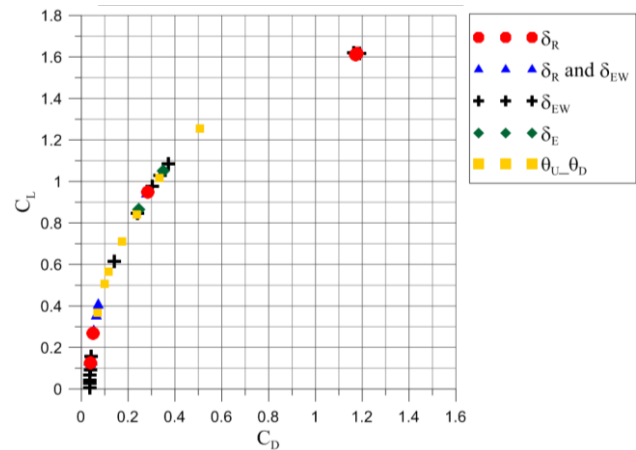


**Fig. 15 Lift versus drag coefficient for trim conditions for  $Re=10.5 \cdot 10^6$**

Derivatives of the lift in respect to the control surfaces deflection versus the angle of attack are presented in Fig. 16.

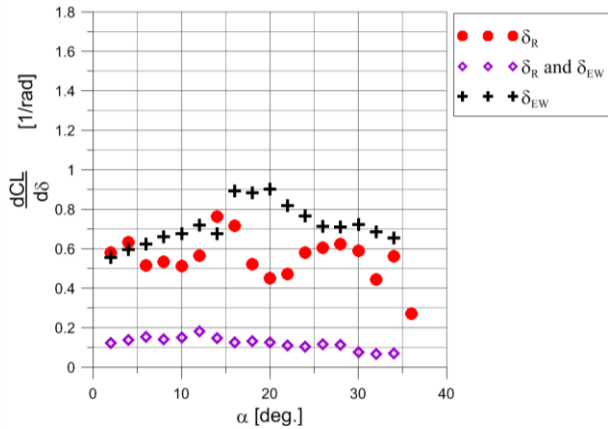


**Fig. 16 Derivative of lift coefficient in respect to control surfaces deflection versus the angle of attack for  $Re=10.5 \cdot 10^6$**

Derivatives of the pitching moment in respect to the control surfaces deflection versus the angle of attack are presented in Fig. 17.

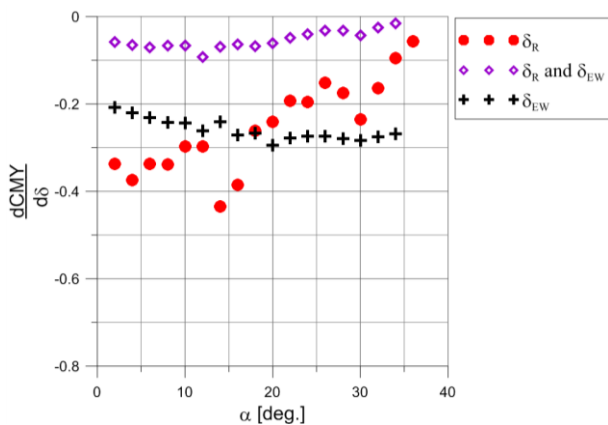


**Fig. 17 Derivative of pitching moment coefficient in respect to control surfaces deflection versus the angle of attack for  $Re=10.5 \cdot 10^6$**

The most effective configuration of control surfaces deflection for small angles of attack is the all moving tail. However for the bigger angles of attack deflection of inner part of the elevon is the most effective configurations.

The less effective is simultaneous deflection of inner part of the elevon and the all moving tail

## 5 Results for supersonic cases

Calculations for supersonic speed was conducted only for one Mach number equal 1.2.

The vortex flow visualization over the Rocket Plane with the all moving tail deflected is presented in Fig. 18.

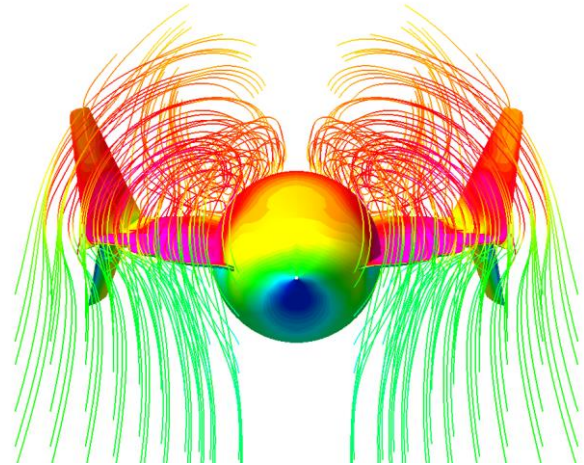


**Fig. 18 Vortex flow visualization for  $Ma=1.2$ ,  $\alpha=26$  deg. and  $\delta_R=-15$**

The pressure coefficient distribution for Rocket Plane with all moving tail deflected is presented in Fig. 19.

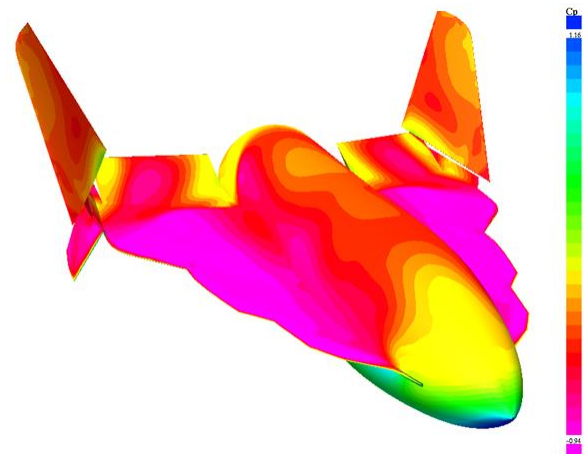


**Fig. 19 Pressure coefficient distribution for  $\alpha=26$  [deg],  $Ma=1.2$  and  $\delta_R=-15$**

### 5.1 Longitudinal static stability

The pitching moment coefficient versus the angle of attack for  $Ma=1.2$  is presented in Fig. 20. The Rocket Plane is longitudinal statically stable for angles of attack between 0 to 26 degrees.

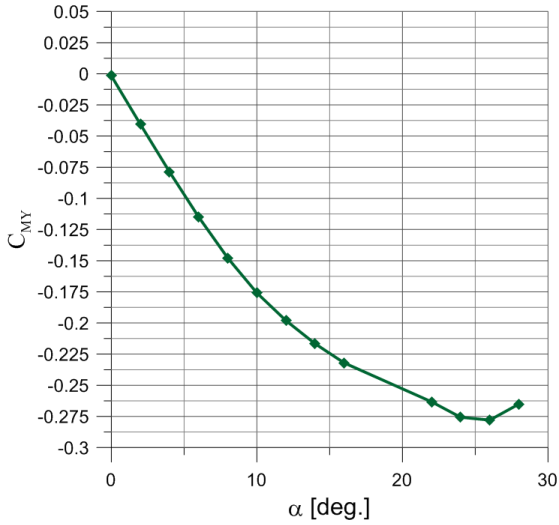


**Fig. 20 Pitching moment coefficient versus angle of attack for Ma=1.2**

**5.2 Control of the pitching channel**

The lift versus drag coefficient for Ma=1.2 is presented in Fig. 21. To obtain the trim conditions three configurations of control surfaces deflection were analyzed:

- The all moving tail ( $\delta_R$ );
- Both segment of the elevons ( $\delta_E$ );
- The all moving tail and both segment of the elevons ( $\delta_R$  and  $\delta_E$ ).

Simultaneous deflection of both parts of the elevons and the all moving tail gives the biggest lift to drag ratio. Moreover, deflection only the elevons or only the all moving tail ensures the equilibrium state only for small angles of attack.

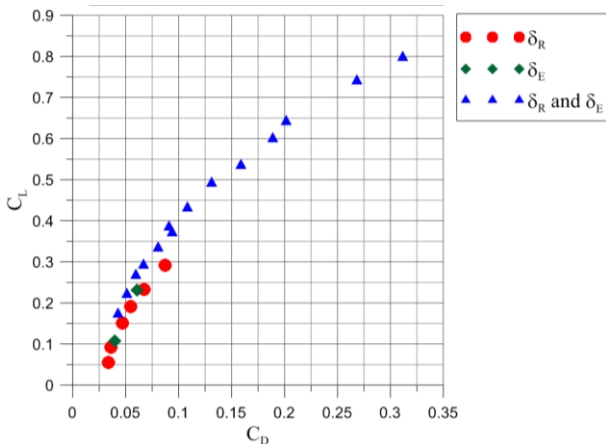


**Fig. 21 Lift versus drag coefficient for trim conditions and Ma=1.2**

Derivatives of the lift in respect to the control surfaces deflection versus the angle of attack are presented in Fig. 22.

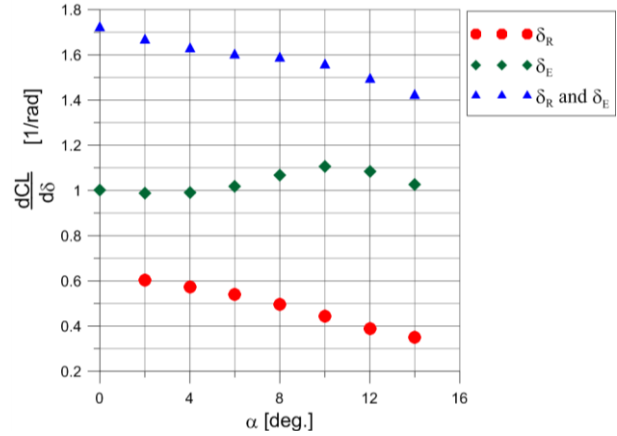


**Fig. 22 Derivative of lift coefficient in respect to control surfaces deflection versus the angle of attack for Ma=1.2**

Derivatives of the pitching moment in respect to the control surfaces deflection versus the angle of attack are presented in Fig. 23.

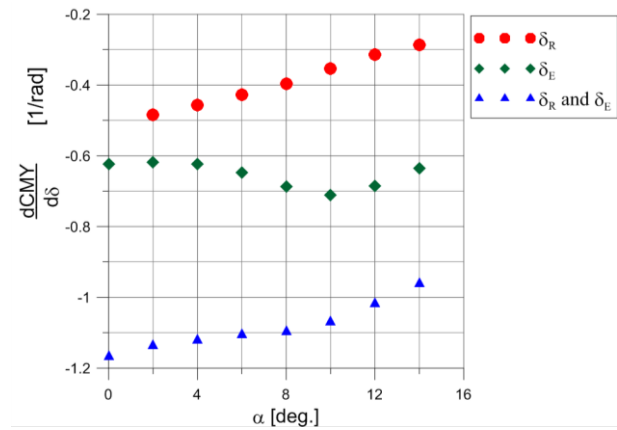


**Fig. 23 Derivative of pitching moment coefficient in respect to control surfaces deflection versus the angle of attack for Ma=1.2**

The most effective configurations of control surfaces deflection is simultaneous deflection of the all moving tail and the elevons. The less effective case is deflection only the all moving tail.

**6 Conclusions**

The longitudinal static stability of the Rocket Plane for subsonic and supersonic

speeds was investigated. The Rocket Plane is stable for subsonic cases and the angle of attack between 0 to 8 degrees and between 28 to 42 degrees (see Fig. 9). Tailless aircraft with a LEX have a problem with stability which is caused by vortex flow generated by the LEX [10]. For supersonic case the Rocket Plane is longitudinal statically stable for the angles of attack between 0 to 26 degrees, which is closed to the critical angle of attack.

The influence of the dihedral of the all moving tail was analyzed. The changing of this parameter do not caused the eliminations of the unstable part of the aerodynamic characteristic. If the all moving tail dihedral is closed to 90 degrees then the range of usability is wider (see Fig. 10).

The most effective configuration of control surfaces deflection for subsonic speeds are simultaneous deflection of the all moving tail and the elevons (see Fig. 12, Fig. 13). However, the all moving tail deflection and inner part of elevons deflection has the less effectiveness case (see Fig. 16, Fig. 17).

The most effective configuration of control surfaces deflection for the supersonic speed are simultaneous deflection of the all moving tail and the elevons. However, the all moving tail deflection has the less effectiveness (see Fig. 16, Fig. 17) compare to other configurations.

The effectiveness of the control surfaces deflection increased in respect to increase in Mach numbers.

The concept of control which involves the rotating side plates (all moving tail) and the two segmented elevons is effective for both subsonic and supersonic speeds. Also changing the all moving tail dihedral can be used to obtain the equilibrium state.

## 7 Further work

It is planned to carry out flight tests of the Rocket Plane and presented concept of control.

## Acknowledgments

This work has been supported by: the National Science Centre through grant no. 2011/01/N/ST8/02525

## References

- [1] The TAURI GROUP *Suborbital Reusable Vehicles: A10-Year Forecast of market Demand*
- [2] Burek R. *Konceptcja stopnia orbitalnego raketoplanu*. Master thesis. *Not published*. 2009
- [3] Galiński C., Goetzendorf-Grabowski T., Mieszalski D., Stefanek Ł. A concept of two-staged spaceplane for suborbital tourism. *Transactions of the Institute of Aviation*, Vol.191, No. 4/2007, pp. 33-42.
- [4] Figat M., Galiński C., Kwiek A. Modular Aeroplane System. A concept and initial investigation. *Proceedings of 28<sup>th</sup> ICAS*, Brisbane, paper number ICAS 2012-1.3.2, 2012
- [5] Figat M., Galiński C., Kwiek A. Aeroplane Coupled System to Space Tourism. *Progress in Aeronautics Vol. 32 No. 1 pp 23-37, 2011*
- [6] Kwiek A. Initial optimization of the strake for the rocket plane. *AIAA Pegasus Student Conference*, Poitiers, 2012
- [7] Kwiek A., Figat M. Study on influence of deflected strake on the rocket plane aerodynamic characteristics. *Proceedings of 4<sup>th</sup> CEAS 2013 Air & Space Conference in Linköping*, paper number 10, pp. 7-16, 2013
- [8] Lamar J.E., Neal Frink N.T. Experimental and Analytical Study of the Longitudinal Aerodynamic Characteristics of Analytically and Empirically Designed Strake-Wing Configuration at Subcritical Speeds. *NASA Technical Paper 1803*
- [9] Mavriplis D.J. Three-Dimensional Unstructured Multigrid for the Euler Equations, *Journal of Aircraft*, Vol. 30, No 7, July 1992
- [10] Brandon J.M. Low-Speed Wind-Tunnel Investigation of the Effect of Strake and Nose Chines on Lateral-Directional Stability of a Fighter Configuration, *NASA Technical Memorandum 87641*, 1986

## Contact Author Email Address

[akwiek@meil.pw.edu.pl](mailto:akwiek@meil.pw.edu.pl)

## Copyright Statement

The authors confirm that they, and/or their company or organization, hold copyright on all of the original material included in this paper. The authors also confirm that they have obtained permission, from the copyright holder of any third party material included in this paper, to publish it as part of their paper. The authors confirm that they

give permission, or have obtained permission from the copyright holder of this paper, for the publication and distribution of this paper as part of the ICAS 2014 proceedings or as individual off-prints from the proceedings.